

Light Microscopic Variation of Fiber Cell Size, Shape and Ordering in the Equatorial Plane of Bovine and Human Lenses

K. J. Al-Ghoul and M. J. Costello¹

Department of Cell Biology and Anatomy, University of North Carolina at Chapel Hill, Chapel Hill, NC 27599-7090

Purpose. A rapid means was sought to visualize and quantify the cross-sectional areas of fiber cells, the variations of cell area, and the regularity of packing in the equatorial plane of normal adult bovine and normal aged human lenses.

Methods. Vibratome sections of bovine and human lenses were fixed, embedded in LR White resin, and sectioned for light microscopic observation. Image analysis was performed to determine the cross-sectional areas of fiber cells in selected nuclear regions.

Results. Examination of bovine lenses revealed a pattern of cell size and shape in each region that was similar to that recently reported for normal human lenses (1). In the equatorial plane of bovine lenses, average cross-sectional areas were $20 \pm 6 \mu\text{m}^2$ in the adult nucleus, $43 \pm 19 \mu\text{m}^2$ in the fetal nucleus, and $63 \pm 61 \mu\text{m}^2$ in the embryonic nucleus. Light microscopy of human lenses was consistent with our previous electron microscopic observations. Moreover, in both bovine and human lenses, the distribution of cell sizes and the number of cell layers was readily available for each region. Overviews of the equatorial plane demonstrated a gradual improvement in the regular packing of radial cell columns proceeding from the relatively disordered embryonic and fetal nuclei through the well-ordered adult nucleus to the highly regular cortical region.

Conclusions. Light microscopy revealed the highly irregular packing and large average size of cells in the embryonic nucleus and the gradual reduction in size and progressive improvements in regularity of packing in the outer layers. The methods used here have the advantage of rapidly giving a continuous view of the fiber cell structure and arrangement which is not available using electron microscopy.

Recent electron microscopic studies have demonstrated that mammalian lens fibers are not homogeneous in size and shape throughout the lens (1-3). While these ultrastructural observations have been critical in formulating a detailed understanding of fiber cell morphology, several important limitations of this technique are apparent. First, only a small percentage of the fiber cells in a particular region can be examined since the area of a thin-section mesa is typically less than 0.25 mm^2 . Second, thin-section mesas raised at intervals along the equatorial plane provide only an intermittent view of fiber cell shape and arrangement. Third, obtaining quantitative measurements of cell size via transmission electron microscopy is a time consuming and laborious process. In order to overcome these limitations we have utilized a light microscopic technique that allows for rapid visualization of all nuclear regions in bovine and human lenses. Because we are able to survey a large number of cells at one time, the quantification process is also simplified.

MATERIALS AND METHODS

Lenses—Adult bovine eyes (approximately 2-3 years old) were obtained from an arbitore immediately after slaughter.

¹To whom correspondence should be addressed: Department of Cell Biology and Anatomy, Rm 518 Taylor Hall, CB7090, University of North Carolina at Chapel Hill, Chapel Hill, NC 27599-7090. Phone: (919) 966-6981; e-mail: mjc@med.unc.edu

The eyes were transported on ice to the laboratory and all lenses were dissected from the globes within 6 hours of death. A total of five bovine lenses were utilized in this study; all were clear and colorless.

Normal aged human lenses were obtained via organ donors (through the North Carolina Eye and Human Tissue Bank, Durham, NC). The lenses were dissected from the globe within 12 hours post mortem, and transported to the laboratory in vials containing gauze moistened with human balanced salt solution. A total of four lenses, aged 59, 59, 65 and 66 years, were obtained. The human lenses were fully transparent and pale yellow in color.

Vibratome sectioning—Before sectioning, the equatorial diameter and anterior-to-posterior height were measured for both human and bovine lenses. The capsule and soft cortical tissue were removed to facilitate Vibratome sectioning and the lens nuclei were mounted on a metal sectioning tray with cyanoacrylate glue. Lenses were covered with warm 2.5% agar, covered with balanced salt solution at 10°C and sectioned using a vibrating knife microtome (TPI Vibratome model 1000, St. Louis, MO) at an amplitude of 7, a speed of approximately 0.2 mm/sec. , and a cutting angle of 12° .

Light Microscopy—Vibratome sections $100\text{-}200 \mu\text{m}$ thick were fixed in 0.5% glutaraldehyde, 2% paraformaldehyde, and 1% tannic acid in 0.1M cacodylate buffer (pH 7.4) for 16-20 hours. Sections were washed 4 x 10 minutes with deionized, distilled water, enbloc stained in 2% aqueous uranyl acetate in dark for 1 hour, washed 1 x 10

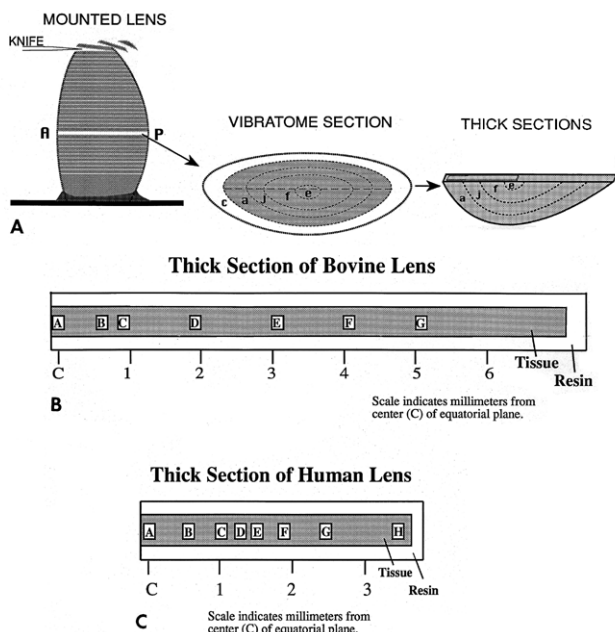


Figure 1. Preparation of thick sections for light microscopy. A. **Vibratome sectioning of lenses.** Lenses were mounted and sectioned parallel to the optic axis. A = anterior pole, P = posterior pole. Vibratome sections at or near the optic axis contained all the developmental regions of the lens: c = cortex, a = adult nucleus, j = juvenile nucleus, f = fetal nucleus, e = embryonic nucleus. Vibratome sections were bisected along the equatorial plane and thick sections (0.5µm to 1.0µm) were cut along 1/2 of the equatorial axis, stained with toluidine blue, and mounted on glass slides for light microscopic examination. B. **Composite diagram of a thick section from a bovine lens.** The location of light micrographs in Figure 2 is shown. C. **Composite diagram of a thick section from a human lens.** The location of light micrographs in Figure 3 is shown.

minutes with deionized, distilled water, then dehydrated through a graded ethanol series. Sections were infiltrated and embedded in LR White resin (Electron Microscopy Sciences, Ft. Washington, PA).

Thick sections (0.5µm to 1.0µm) were cut along one-half of the equatorial axis (Fig. 1A) and mounted on glass slides. Mounted sections were stained with toluidine blue, cover slipped, then examined with an Olympus BX40 light

microscope. Images were recorded with an Olympus PM20 35 mm camera. Figures 1B and 1C are diagrams of the thick sections from bovine and human lenses, respectively. The location of photographs in Figures 2 and 3 are shown.

Image Analysis—Negatives were illuminated with a DC high intensity light source (Gordon Instruments, Orchard Park, NY) and scanned using an Eikonix 1412 scanning CCD camera (Ektron, Bedford, MA) at a pixel resolution of 2048 X 2048. A reticle (model no. 7, Ted Pella, Redding, CA) was placed on each negative during scanning for use as a calibration tool. Images were scanned and recorded using Adobe Photoshop v. 2.5 (Adobe Systems, Mountain View, CA) on a Macintosh Centris 650 computer (Apple Computers, Cupertino, CA).

Morphometry was performed on bovine and human lenses using NIH Image v. 1.53 (4). The cross-sectional area of at least 75 fiber cells was measured in each of three regions in bovine lenses, i.e. the adult nucleus, the fetal nucleus and the embryonic nucleus, and in the fetal and embryonic regions of human lenses. Adult nuclear fiber cells in human lenses could not be measured at the light-microscopic level due to the extensive compression of cell profiles in the outer nucleus.

RESULTS

Normal Bovine Lenses—Nuclear fiber cells in all the bovine lenses were intact and showed no evidence of disruption or damage (Fig. 2). In the equatorial plane, a continuous view of fiber cell size and arrangement was available. Because all the fibers were cut cross-sectionally, comparisons were easily made between the nuclear regions.

The embryonic nucleus contained the largest fiber cell profiles (Fig. 2A) as well as the largest variation in cross-sectional area. The average cross-sectional area was 63 ± 61µm² (see Table I for complete morphometric results). Fiber cell packing was disordered, with no discernible radial cell columns.

In the fetal nuclear region, gradual changes in fiber cell size, shape and arrangement were noted along the equatorial plane (Fig. 2, B-D). Fetal cells adjacent to the embryonic region (0.6 µm from center) varied greatly in size. These earliest secondary fibers displayed rounded profiles and a disordered arrangement (Fig. 2B). Short, irregular rows of fibers were noted approximately 1 µm from the lens center

TABLE I:
Morphometry of Bovine and Human Lens Cells from Light Microscopy

Developmental Region	Reference Micrograph	Number of Cells Measured	Ave. Area ± SD (µm ²)
Bovine			
Embryonic Nucleus	Fig. 2A	75	63 ± 61
Fetal Nucleus	Fig. 2C	75	43 ± 19
Adult Nucleus	Fig. 2F	88	20 ± 6
Human			
Embryonic Nucleus	Fig. 3A	76	92 ± 76
Fetal Nucleus	Fig. 3C	78	38 ± 18

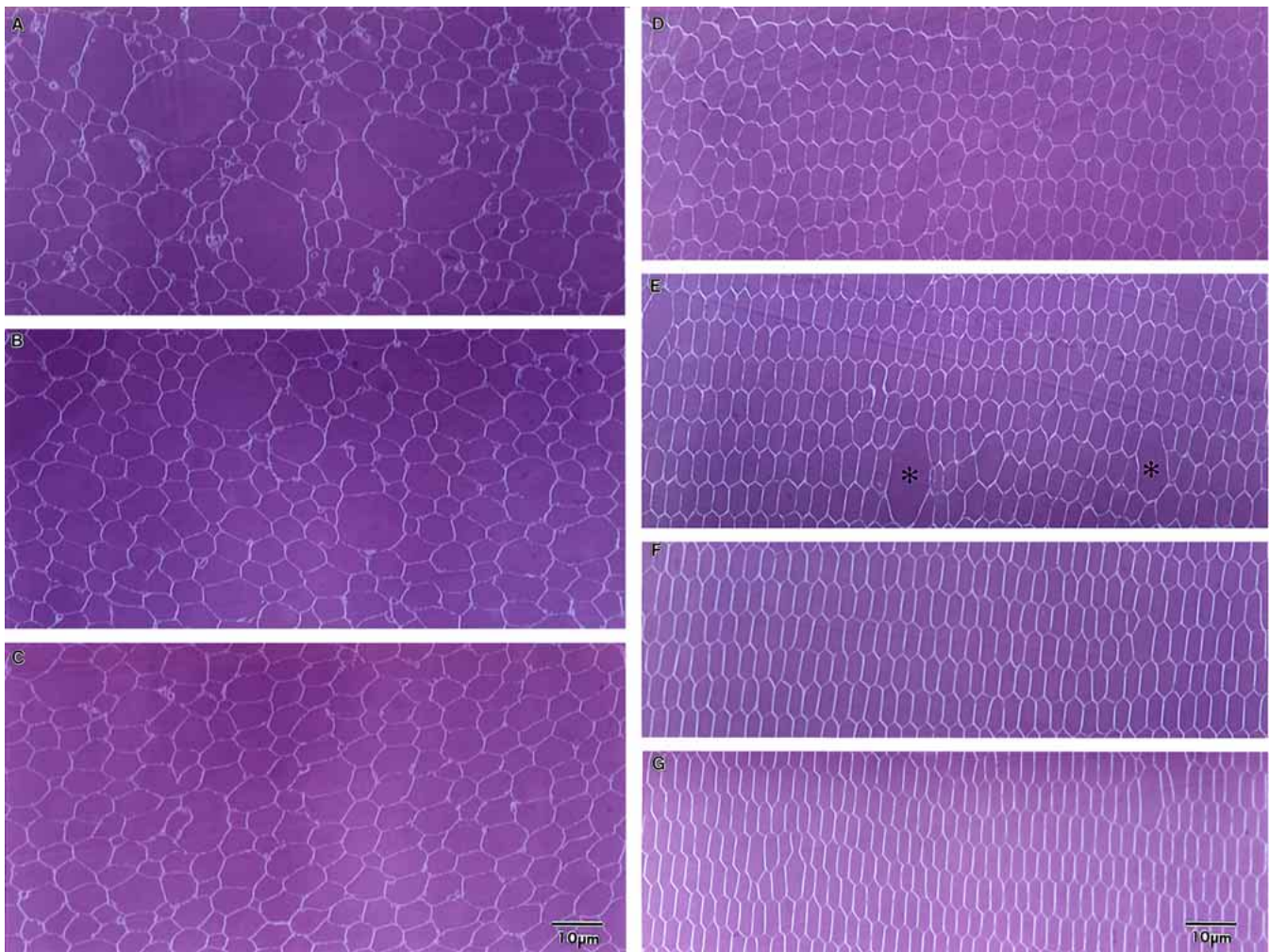


Figure 2. Light micrographs of bovine nuclear fiber cells in the equatorial plane. A. Embryonic nucleus. The largest cells are found in the embryonic nucleus, where the disordered packing and large range in cross-sectional area is apparent. Location = center of the equatorial plane. **B-D. Fetal Nucleus.** Panels B-D display how the cell size, shape and arrangement gradually changes from disordered, rounded profiles which vary greatly in size (B), to flattened hexagonal profiles of more uniform size (D). Short irregular rows are discernible in C, which become easily recognizable radial cell columns in D. **B.** Location = 0.6 mm from lens center. **C.** Location = 1 mm from the lens center. **D.** Location = 2 mm from the lens center. **E. Juvenile Nucleus.** The juvenile nuclear region is characterized by occasional large profiles interspersed among relatively uniform fiber cells arranged in regular radial cell columns. Location = 3 mm from the lens center. **F-G. Adult Nucleus.** Fiber cells of the adult nucleus (F-G) are highly flattened hexagons in shape and display very regular packing. Cell profiles in figure G (located 5 mm from the lens center) appear more flattened than those in figure F (located 4 mm from the lens center).

(Fig. 2C), where fiber profiles were smaller and more uniform in size. The average cross-sectional area of fetal nuclear fibers at this location was $43 \pm 19 \mu\text{m}^2$ (Table I). At about 2 mm from the center (Fig. 2D), fiber cells were arranged in irregular radial cell columns. Both rounded profiles and flattened, hexagonal profiles were common at this location. A further reduction in cross-sectional area was noted.

In general, fiber cells in the juvenile nuclear region were uniform in size and shape (Fig. 2E). Flattened, hexagonal profiles were arranged in easily recognizable radial cell columns. Large fiber cell profiles spanning 2-3 radial cell columns (Fig. 2E, asterisks) were commonly interspersed between the smaller cells at this location (approximately 3 mm from the lens center).

In the adult nuclear region, fiber cells were highly flattened hexagons arranged in regular radial cell columns (Fig. 2, F-G). The cross-sectional area of fibers at

approximately 4.0 mm from the lens center was $20 \pm 6 \mu\text{m}^2$ (Table I). Fiber profiles appeared more flattened at 5.0 mm from the lens center than at 4.0 mm from the lens center (compare Fig. 2F and 2G). The size, shape and arrangement of fiber cells located 5-7 mm from the lens center were indistinguishable from those displayed in Fig. 2G.

Normal Human Lenses—Light microscopic examination of normal aged human lenses gave an overview of lens fiber morphology that was consistent with our previous detailed electron microscopic observations (1,3). Along the equatorial plane, fiber cells were undisrupted and demonstrated a gradual reduction in size proceeding from the embryonic nucleus through the adult nucleus (Fig. 3, A-H).

In the embryonic (Fig. 3A) and inner fetal (Fig. 3B) regions, fiber cell profiles were rounded, highly variable in size, and randomly arranged. Embryonic fiber cells had an average cross-sectional area of $92 \pm 76 \mu\text{m}^2$. At approximately 1 mm from the lens center, fetal nuclear cells



Figure 3. Light micrographs of aged human nuclear fiber cells in the equatorial plane. A. Embryonic Nucleus. The primary fiber cells in humans are quite similar to bovine primary fibers in both size and arrangement. Location = center of the equatorial plane. **B-F. Fetal nucleus.** In the fetal nucleus (B-E), considerable reduction in cross-sectional size is evident as regions further from the lens center are examined. The rounded profiles (B-C) gradually become flattened and irregular (D-F), but do not have the hexagonal shape seen in bovine lenses. Short rows of cells (C) become organized into radial cell columns (E), however, these are more difficult to discern in the human than in the bovine. The fibers continue to flatten (F) and the profiles take on an undulating appearance which is also seen in panels G and H. **B.** Location = 0.6 mm from the lens center. **C.** Location = 1 mm from the lens center. **D.** Location = 1.3 mm from the lens center. **E.** Location = 1.5 mm from the lens center. **F.** Location = 2 mm from the lens center. **G. Juvenile Nucleus.** Two distinct cell sizes are characteristic of the juvenile nuclear region, where larger cells are interspersed among the highly flattened cell profiles. Location = 2.4 mm from the lens center. **H. Adult Nucleus.** Cells of the adult nuclear region are highly compressed, making their profiles difficult to distinguish. Location = 3.5 mm from the lens center.

appeared more uniform in size and were arranged in short, irregular rows (Fig. 3C). The cross-sectional area was $38 \pm 18 \mu\text{m}^2$. The fiber profiles gradually became more flattened in the fetal regions 1-2 mm from the lens center (Fig. 3, D-F). In this region, cell profiles were arranged in irregular radial cell columns. At the outermost region of the fetal nucleus (Fig. 3F) flattened fiber profiles displayed an undulating appearance, which was also noted in the juvenile (Fig. 3G) and adult (Fig. 3H) nuclear regions. Fiber cells of the juvenile and adult nuclear regions appeared highly compressed; individual profiles could not be distinguished.

DISCUSSION

Light microscopic overviews of bovine and human lens nuclei confirmed that our previous ultrastructural examinations of mammalian lenses were representative of nuclear fiber cell structure in the equatorial plane. The structural features noted in the present investigation were completely consistent with previous electron microscopic

observations of bovine and human lens nuclei (1-3) and with light microscopic observations of frog lenses (5). The results of this study also provide a more continuous view of the cross-sectional size, shape, and arrangement of nuclear fiber profiles than can be obtained using ultrastructural techniques.

Overall, the nuclear fibers of bovine and human lenses were similar in size and arrangement, particularly the embryonic and early fetal fibers. However, the shape of bovine and human nuclear fibers was quite different in the adult, juvenile, and outer fetal regions. While bovine fiber profiles appeared as flattened hexagons, human fibers in comparable regions were extensively compressed and irregular in shape. This is probably due to age-related changes such as condensation and compression that occur in aged primate lenses (6-7).

Another notable difference between bovine and human nuclear lens fibers was the complexity of cell borders. While bovine fibers from the embryonic and fetal nuclear regions had smooth borders, human fiber profiles from comparable

regions displayed many interdigitations. It is well established that mammalian fiber membranes undergo significant age-related alterations that result in increasingly complex cell-cell interdigitations (8). The greater complexity in human cell profiles is presumably due in part to their greater age.

Morphometric analysis of normal human lenses compared quite favorably with data from bovine lenses (Table I). In the embryonic region, both human and bovine profiles had a large average area and a large standard deviation. Since this was seen in both young (2-3 year old bovine) lenses as well as old (59-66 year old human) lenses, it would appear that primary fibers are produced as a non-uniform population. That is, the variable size, shape, and arrangement of cells in the embryonic nucleus is not due to age-related changes. The average cross-sectional area of fetal and adult nuclear fiber cells was greater in bovine lenses than in human lenses. However, this is not surprising, considering the flattened appearance of human fiber cells in the adult region. The fact that human fiber cells in the fetal region also have a smaller area indicates that they are probably subject to some amount of condensation and compression.

The preparative method developed for this study represents a technical advance in light microscopy of lens tissue. Because LR White resin is water soluble, staining of thick sections can be easily and reliably reproduced. This contrasts with hydrophobic resins such as epoxy, which often produce uneven staining and poor contrast in lens tissue. The dense protein matrix of lens fiber cytoplasm was stained, while the membranes and extracellular space were not stained and were seen in negative contrast. This property makes the methodology especially suitable for visualization of cross-sectioned fibers. While the resolution obtained was remarkable for light microscopy, TEM is essential in order to confirm structural details, such as the types of fiber interdigitations and the frequency of fiber junctions. In addition, the fixation and embedding procedures were compatible with immunolabeling, allowing the same tissue to be used for more than one analysis.

Since many fiber cell profiles could be visualized at one time, the technique presented here provides a rapid means of quantifying the cross-sectional areas of fiber cells. This technique should be valuable in making comparisons between cataractous and normal lenses in a variety of animal models as well as in humans.

Acknowledgements—The authors thank the North Carolina Eye and Human Tissue Bank, Durham, NC for providing normal human lenses. This work was supported by Grant EY08148 (MJC) from The National Eye Institute, National Institutes of Health, Bethesda, MD. This work was presented in part at the Annual Meeting of the Association for Research in Vision and Ophthalmology (ARVO), Sarasota, FL, April 1996 (9).

REFERENCES

1. Taylor, V. L., Al-Ghoul, K. J., Lane, C. W., Davis, V. A., Kuszak, J. R. and Costello, M. J. (1996) Morphology of the normal human lens. *Invest Ophthalmol Vis Sci* 37, 1396-1410.
2. Oliver, T.N., Al-Ghoul, K.J., Lane, C.W. and Costello, M.J. (1992) Architecture of fiber cells from nuclei of adult bovine and human lenses. Eleventh Annual Symposium on Advances in Microscopy, Pine Knoll Shores, NC, September 25-27, 1992.
3. Al-Ghoul, K. J. and Costello, M. J. (1996) Fiber cell morphology and cytoplasmic texture in cataractous and normal human lenses. *Curr Eye Res* 15, 533-542.
4. Rasband, W. (1989). Image v1.21, user's guide, PB90-123308. National Institutes of Health, Bethesda.
5. Kuszak, J. R. and Rae, J. L. (1982) Scanning electron microscopy of the frog lens. *Exp. Eye Res.* 35, 499-519.
6. Kuszak, J. R., Ennesser, C. A., Umlas, J., Macsai-Kaplan, M. S. and Weinstein, R. S. (1988) A model for studying membrane senescence. *J Ultrastruc Mol Struc Res* 100, 60-74.
7. Costello, M. J., Oliver, T. N. and Cobo, L. M. (1992) Cellular architecture in age-related human nuclear cataracts. *Invest Ophthalmol Vis Sci* 33, 3209-3227.
8. Kuszak, J. R. and Brown, H. G. (1994) Embryology and anatomy of the lens. In *Principles and Practice of Ophthalmology: Basic Sciences* (Eds. Albert, D. and Jakobiec, F.). Pp. 82-96, WB Saunders Co., Philadelphia.
9. Al-Ghoul, K.J., Taylor, V. L. and Costello, M.J. (1996) Continuous variation of fiber cell size, shape and ordering in the equatorial plane of bovine lenses. *Invest Ophthalmol Vis Sci* 37, S893.